NATIONAL ADVISORY COMMITTEE FOR AERONAUTICS

WARTIME REPORT

ORIGINALLY ISSUED
November 1942 as
Confidential Bulletin

INVESTIGATION OF THE VARIATION OF LIFT COEFFICIENT WITH REYNOLDS NUMBER AT A MODERATE ANGLE OF ATTACK ON A LOW-DRAG AIRFOIL

By Albert E. von Doenhoff and Neal Tetervin

Langley Memorial Aeronautical Laboratory
Langley Field, Va.

NACA

WASHINGTON

NATIONAL ADVISORY COMMITTEE FOR AERONAUTICS

CONFIDENTIAL BULLETIN

INVESTIGATION OF THE VARIATION OF LIFT COEFFICIENT WITH REYNOLDS NUMBER AT A MODERATE ANGLE OF ATTACK ON A LOW-DRAG AIRFOIL

By Albert E. von Doenhoff and Neal Tetervin

SUMMARY

An investigation of the boundary layer about the NACA 66,2-216, a = 0.6, airfoil section has been made in the NACA two-dimensional low-turbulence tunnel, in an attempt to find an explanation for the decreased slope of the lift curve observed for some of the low-drag sections outside the low-drag range at low Reynolds numbers. It was found that the effect was probably associated with the formation of a small local region of separated flow near the leading edge, which decreased in size as the Reynolds number increased.

INTRODUCTION

It has been noticed that the curves of lift coefficient against angle of attack for some of the low-drag sections were not straight outside the low-drag range, particularly at low Reynolds numbers. At Reynolds numbers in the flight range the lift curve became more nearly straight.

In order to determine the cause of the variation of lift coefficient with Reynolds number at moderate angles of attack, the effect was investigated for a representative low-drag airfoil, the NACA 66,2-216, a = 0.6. The investigation, which was carried out in the NACA two-dimensional low-turbulence tunnel, consisted of boundary-layer and lift measurements through a range of Reynolds numbers from 0.9×10^6 to 2.6×10^6.

Changes in lift and boundary-layer characteristics were observed at an angle of attack α of 10.1°, which

was chosen in order that a fairly large change of lift coefficient with Reynolds number would occur. This angle of attack, however, was definitely below that for maximum lift.

APPARATUS

The tests were made in the NACA two-dimensional low-turbulence tunnel, which has a test section 3 feet wide, 7½ feet high, and 7½ feet long. The two-dimensional low-turbulence tunnel has a turbulence level of the order of a few hundredths of 1 percent, as indicated by a hot-wire anemometer.

The lift of the airfoil was measured by observing the change in the pressures on the floor and on the ceiling of the test section. A correction obtained theoretically is applied to the measured results to take into account the finite size of the test section. Lift coefficients obtained in this manner are in good agreement with those obtained in the usual way from pressure-distribution measurements.

The NACA 66,2-216, a = 0.6, airfoil used in this investigation had a chord of 2 feet and a span of 3 feet and entirely spanned the tunnel. The model was constructed of wood with the grain running in the chordwise direction to minimize any unfairness caused by uneven shrinking and swelling of the laminations. The surface of the airfoil was finished with several coats of pyroxylin primer surfacer, wet-sanded using rubber blocks.

The boundary-layer measurements behind 2½ percent of the chord were made with a "mouse" that consisted of a group of four total-pressure tubes and one static-pressure tube. The tubes were made of steel hypodermic tubing that had an outside diameter of 0.040 inch and a wall thickness of 0.003 inch. The total-pressure tubes were flattened at the ends until the opening at the mouth of the tube was 0.006 inch high. A mouse one-half as large as the one just described was used for measurements at 2½ percent of the chord and forward where the boundary layer was especially thin. The arrangement was similar to that described in reference 1.

METHOD

The NACA 66,2-216, a = 0.6, airfoil section was set at an angle of attack of 10.1° and the lift was measured at Reynolds numbers of 0.9, 1.5, 2.2, 2.5, and 2.6 × 10^6. Values of the lift were corrected for tunnel wall effect.

The velocity distributions in the boundary layer were obtained by measuring the static pressure at a point outside the boundary layer and the total pressure at several positions within the boundary layer. The total pressure outside the boundary layer was used as the reference pressure. From these measurements, the ratio of the velocity in the boundary layer to the free-stream velocity was calculated as

$$\frac{u}{U_o} = \sqrt{\frac{h - p}{q_o}}$$

where

u velocity inside boundary layer

U_o free-stream velocity

p local static pressure

h total pressure inside boundary layer

q_o free-stream dynamic pressure

The heights of the total-pressure tubes above the surface were measured with a micrometer microscope.

The pressure distributions were obtained at the same time the boundary-layer measurements were taken by using the measured values of the local static pressure.

$$\left(\frac{U}{U_o}\right)^2 = \left(\frac{H - p}{q_o}\right) = 1 - \left(\frac{\Delta p}{q_o}\right)$$

where

H free-stream total pressure which is constant throughout test section except in boundary layer and wake

U local velocity outside boundary layer

Δp difference between local static pressure and free-stream static pressure

The distances of the boundaries of the region of laminar separation from the wing surface were determined by noting the speed at which each total-pressure tube in the boundary layer first showed a total pressure greater than the local static pressure. Plots were then made of the height of the region of laminar separation at a particular chord position against speed. From these plots, the boundaries of the region of laminar separation for the standard Reynolds numbers were determined.

The thickness of the boundary layer δ is defined as the distance y perpendicular to the surface for which $\left(\frac{u}{U_o}\right) = 0.707 \left(\frac{U}{U_o}\right)$. The thickness δ is determined from the boundary-layer velocity profile for the particular station under consideration. The angle of attack was fixed at 10.1° in the tunnel. This particular angle was chosen because a fairly large change in lift coefficient through the Reynolds number range was observed. The angle, however, was not so high as to cause the flow to be on the verge of complete breakdown.

RESULTS AND DISCUSSION

The phenomenon under investigation is illustrated in figure 1, which shows the variation in the shape of the lift curve with Reynolds number. The variation of section lift coefficient with Reynolds number at a constant angle of attack of 10.1° is shown in figure 2. It is seen that the results of the tests in the two-dimensional low-turbulence pressure tunnel (designated TDT) and in the two-dimensional low-turbulence tunnel (designated LTT) are in good agreement. The slope of the curve decreases with increasing Reynolds number, an indication that the effect under investigation becomes less pronounced as the Reynolds number increases.

The pressure distribution over the upper surface of the airfoil for several Reynolds numbers is given in figure 3. The flat region near the trailing edge indicates

that separation has occurred. It is to be noted that the pressure in the separated region remains constant independent of the Reynolds number; whereas the pressures over the remainder of the upper surface decrease with increasing Reynolds number. Pressures were also measured at a chordwise position x/c of 0.30 on the lower surface and the value of $\left(\frac{U}{U_o}\right)^2$ was found to vary from 0.83 at $R = 0.9 \times 10^6$ to 0.79 at $R = 2.6 \times 10^6$. The increase in lift of the section with increasing Reynolds number is therefore seen to be connected directly with a decrease in pressure over the upper surface and an increase in pressure over the lower surface.

Velocity distributions in the boundary layer for various chordwise positions x/c are given in figures 4 to 6. The variation of the boundary-layer thickness with chordwise position is shown in figure 7. Figure 8 shows the relative thickness of the boundary layer at $\alpha = 10.1^\circ$ as compared with the airfoil dimensions and the large increase in thickness associated with separation. The velocity profiles near the leading edge indicate the existence of a local region of separated flow. The extent of this region and the pressure distribution near the leading edge are shown in figure 9.

In order to obtain more information regarding the separated region near the leading edge, a suspension of lampblack in kerosene was painted on the wing in each case before the tunnel was started. (See fig. 10(a).) When the air stream was started, the fluid collected in the separated region. The flow patterns were photographed while the tunnel was running. It is seen from figures 10(b) to 10(e) that the extent of the separated region decreased as the Reynolds number increased. This result is in agreement with the conclusions drawn from the boundary-layer surveys.

A qualitative picture of the mechanism that brought about the observed variation of lift coefficient with Reynolds number in this case is suggested by the experimental results obtained in this investigation. When partial stalling of the flow near the trailing edge occurs, there is no reason to suppose that the circulation and hence the lift coefficient is determined by the Kutta-Joukowski condition. It was found in this case that the pressure in the separated region remained substantially constant, independent of the Reynolds number, at a value

slightly below that of free-stream static pressure. Examination of numerous pressure-distribution data shows that the pressure in a region of permanent separation is relatively insensitive to changes in flow about the airfoil and usually has a value similar to that observed in this case. The condition that the pressure in the separated region remains substantially constant is not in itself sufficient to determine the circulation, because the point along the airfoil surface at which this pressure is attained is not yet determined. If in addition to the pressure in the separated region, however, the amount of pressure recovery from the leading edge is known, then the circulation and the position of the final separation point is determined.

Consideration of the effect on the pressure distribution of variation in the circulation shows that these conditions are sufficient to determine the flow. It is assumed that the angle of attack is fixed and that separation occurs at a fixed value of the pressure coefficient corresponding to a pressure a little less than free-stream pressure. If the circulation is then increased, the pressures on the upper surface near the leading edge must decrease. Consequently, the amount of pressure recovery which occurs before the flow separates increases with increase in the circulation; that is, the pressure recovery is a function of the circulation. For a given airfoil at a given angle of attack, therefore, the circulation is determined if the amount of pressure recovery is specified in addition to the pressure in the separated region.

The pressure recovery from the leading edge takes place almost entirely in a region covered by the turbulent boundary layer. The amount of pressure which can be recovered with a turbulent boundary layer is mainly a function of its initial thickness; that is, the thinner the initial thickness of the turbulent boundary layer, the greater the pressure difference between the point where the boundary layer begins and the point where it separates. Hence, a decrease in the boundary-layer thickness near the leading edge must correspond to an increase in the lift coefficient when the flow over the airfoil is partially stalled.

In the case under consideration, the turbulent boundary layer is affected by the Reynolds number in two ways. The first effect is the normal decrease in thickness of the turbulent boundary layer associated with an increase in Reynolds number. The second and more important effect

in the present case is the large decrease in the initial thickness of the turbulent boundary layer where it forms just at the end of the region of laminar separation. (See fig. 11.) The thickness of the initial turbulent boundary layer is largely determined by the size of the preceding region of laminar separation which decreases rapidly with increase in Reynolds number.

At higher Reynolds numbers it seems likely that the region of local separation near the leading edge will become insignificant or will completely disappear. It is to be expected then that the lift may continue to increase somewhat with increase in Reynolds number, owing to the normal decrease in boundary-layer thickness with increasing Reynolds number, but at a considerably lower rate.

Langley Memorial Aeronautical Laboratory,
National Advisory Committee for Aeronautics,
Langley Field, Va.

REFERENCE

1. Jones, B. Melvill: Flight Experiments on the Boundary Layer. Jour. Aero. Sci., vol. 5, no. 3, Jan. 1938, pp. 81-94.

ERRATA ON FIGURES

The values of section lift coefficient obtained from TDT test 90 (figs. 1 and 2) should be corrected by the following equation

$$c_{l\,(\text{corrected})} = 0.964c_l + 0.008$$

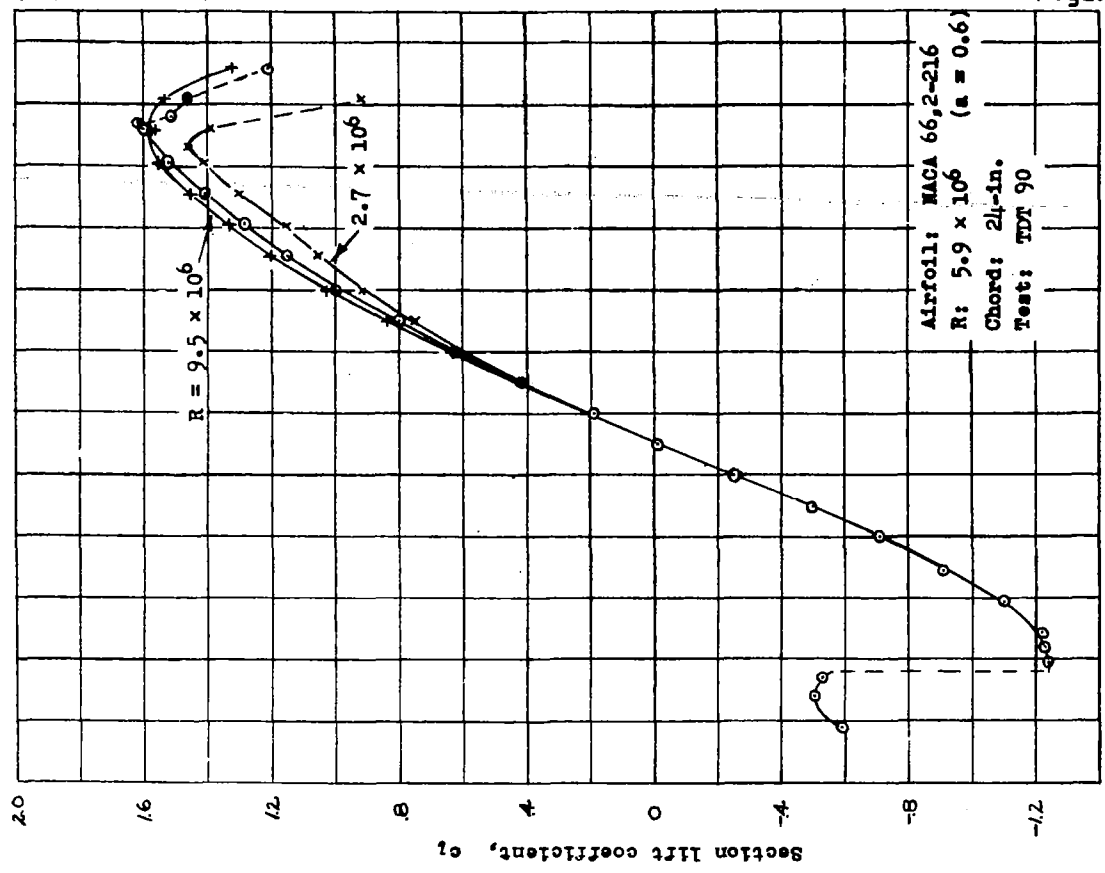

Figure 1.- Variation in lift-curve shape with Reynolds number. NACA 66,2-216, a = 0.6, airfoil section.

δ Boundary-layer thickness

Line where the dynamic pressure inside the boundary layer is equal to 2 percent of the dynamic pressure outside the boundary layer

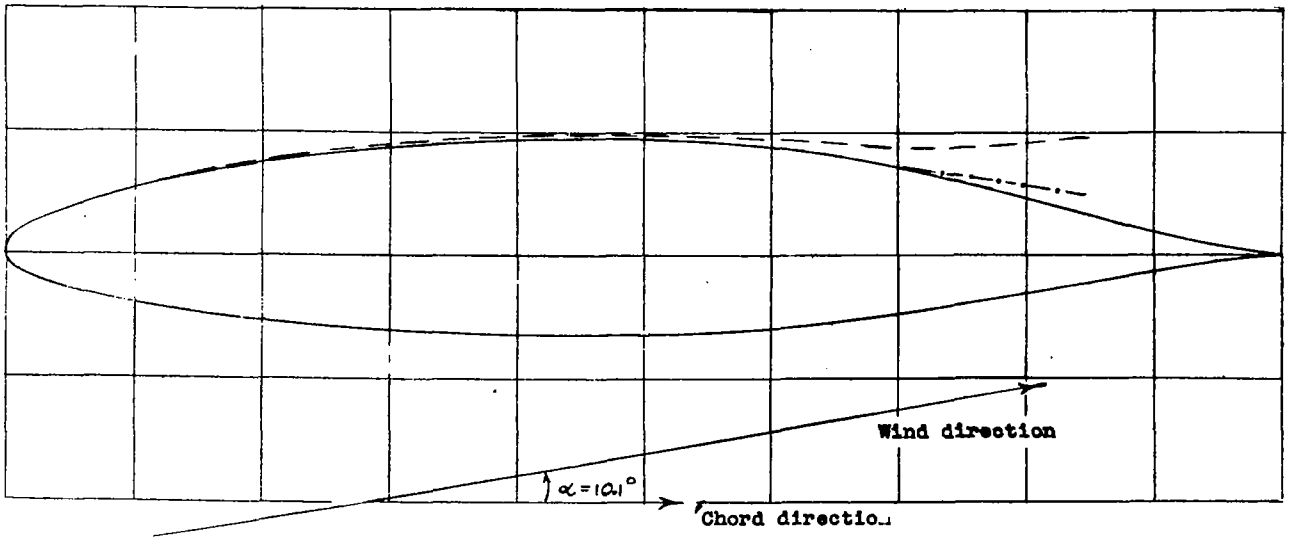

Figure 8.- Boundary-layer thickness on upper surface of NACA 66,2-216, a = 0.6, airfoil section. R, 2.6 x 10^6.

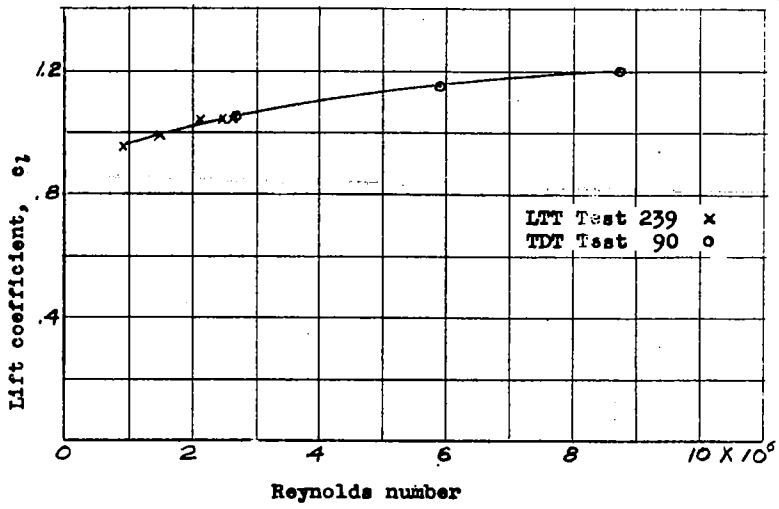

Figure 2.- Variation of section lift coefficient with Reynolds number. NACA 66,2-216, a = 0.6, airfoil section; α, 10.1°.

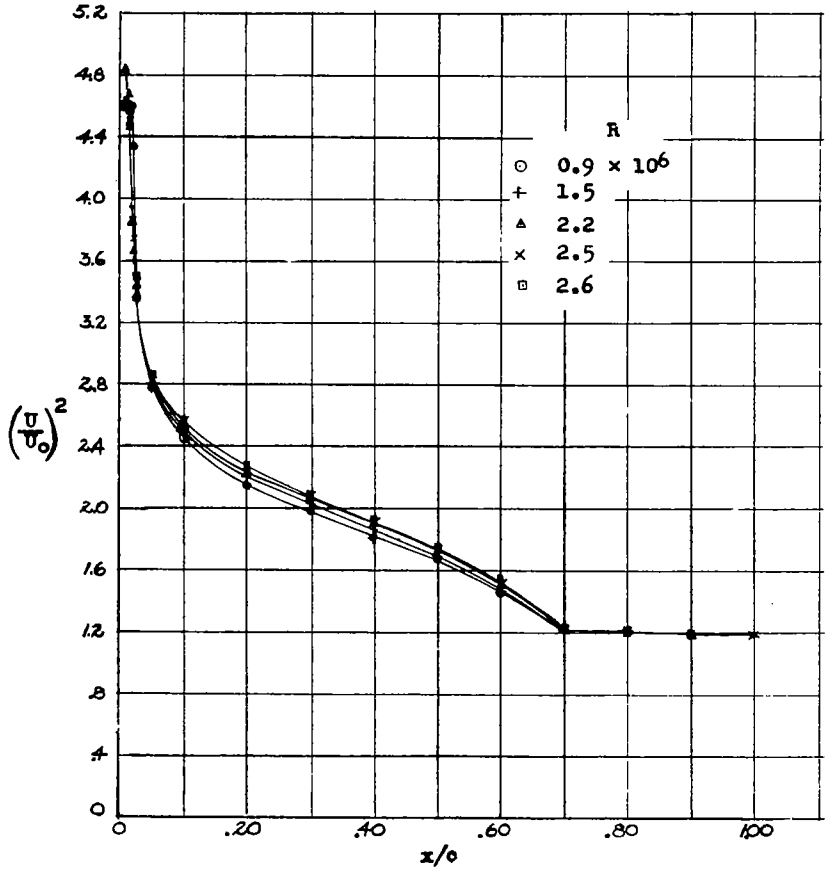

Figure 3.- Upper-surface pressure distributions for several Reynolds numbers. NACA 66,2-216, a = 0.6, airfoil section; α, 10.1°.

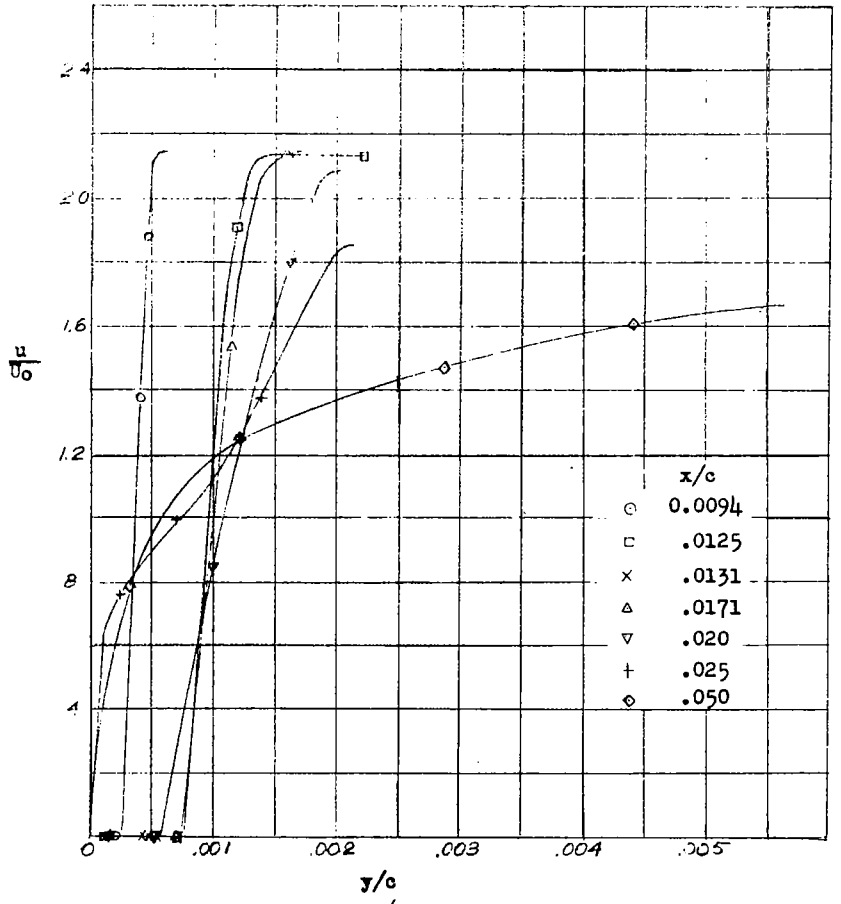

(a) R, 0.9×10^6.

(a-d) Figure 4.- Boundary-layer velocity profiles in the region forward of the 10-percent-chord station. NACA 66,2-216, a = 0.6, airfoil section; α, 10.1°.

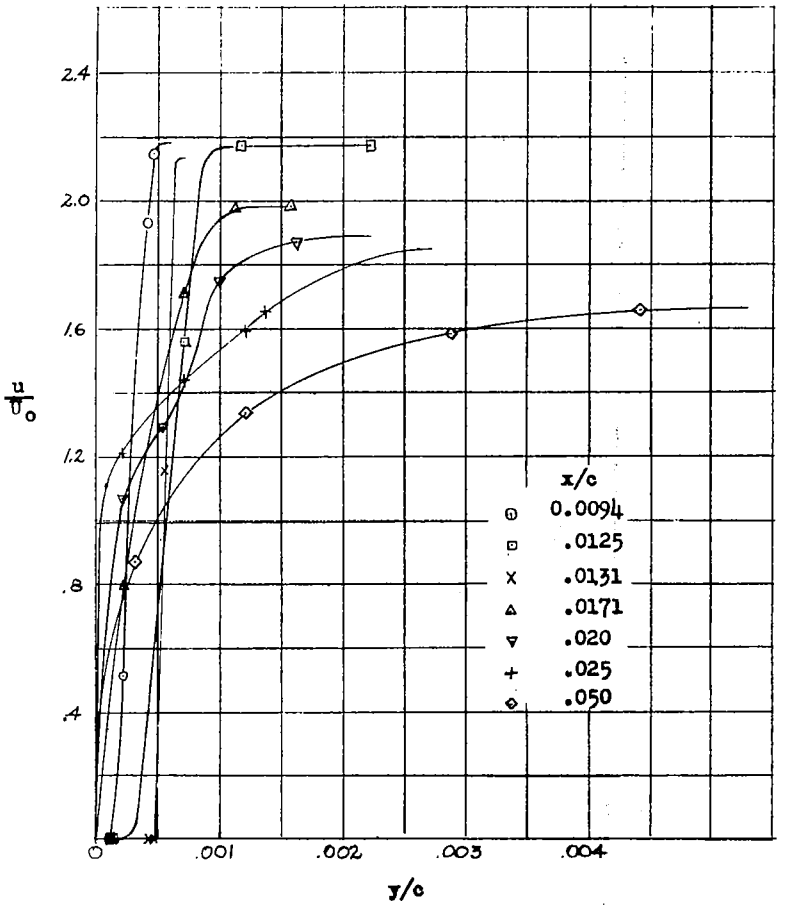

(b) R, 1.5×10^6.

Figure 4.- Continued.

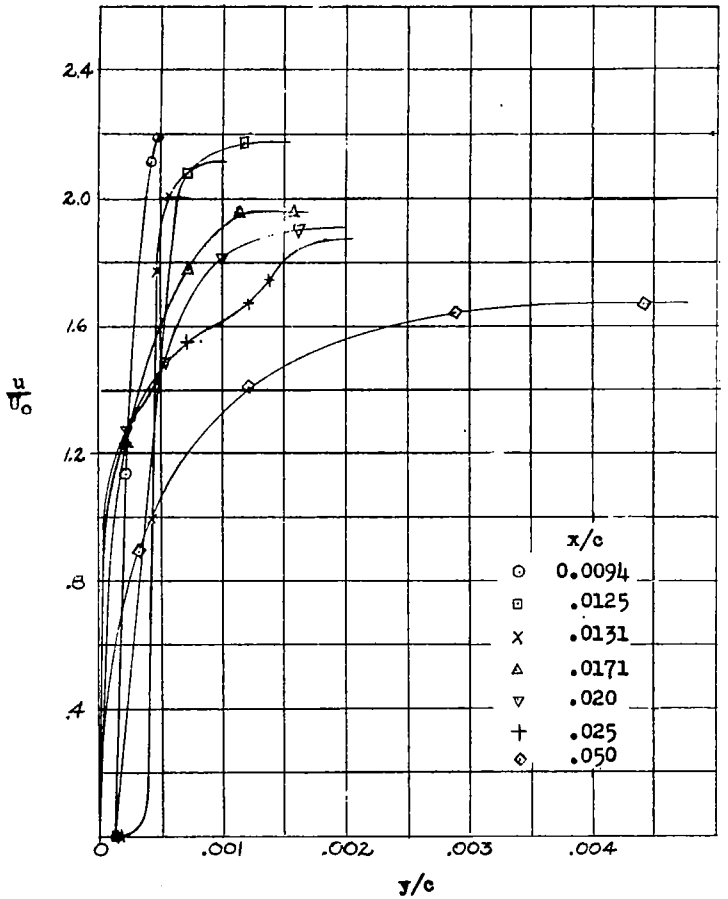

(c) R, 2.2×10^6.

Figure 4.- Continued.

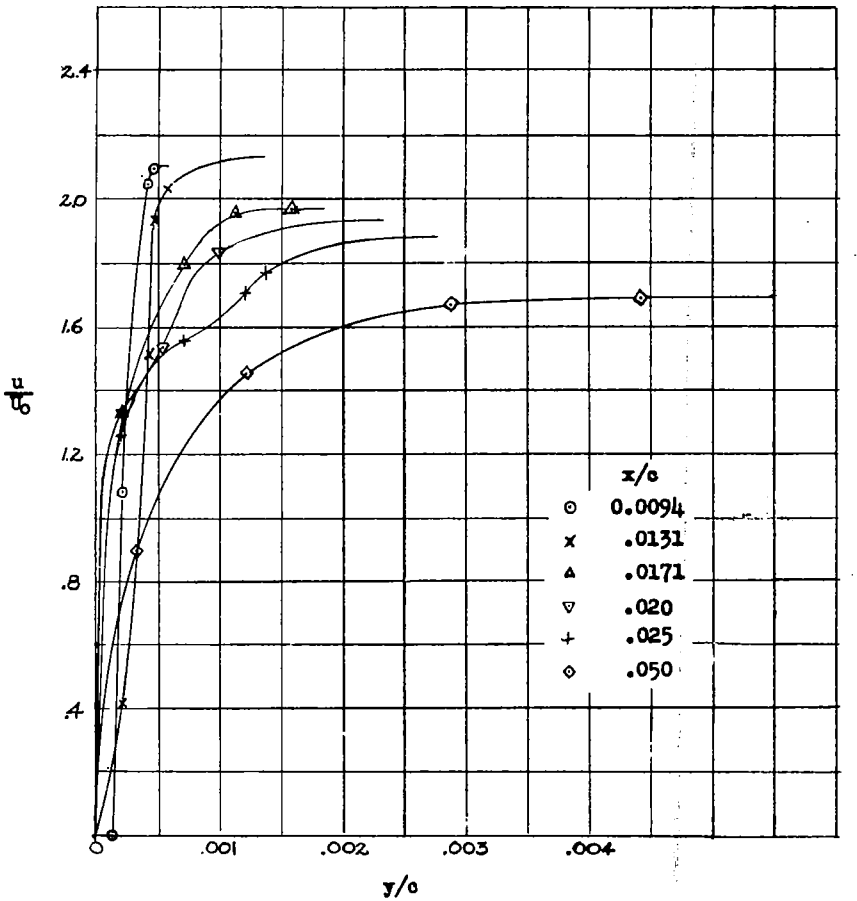

(d) R, 2.5×10^6.

Figure 4.- Concluded.

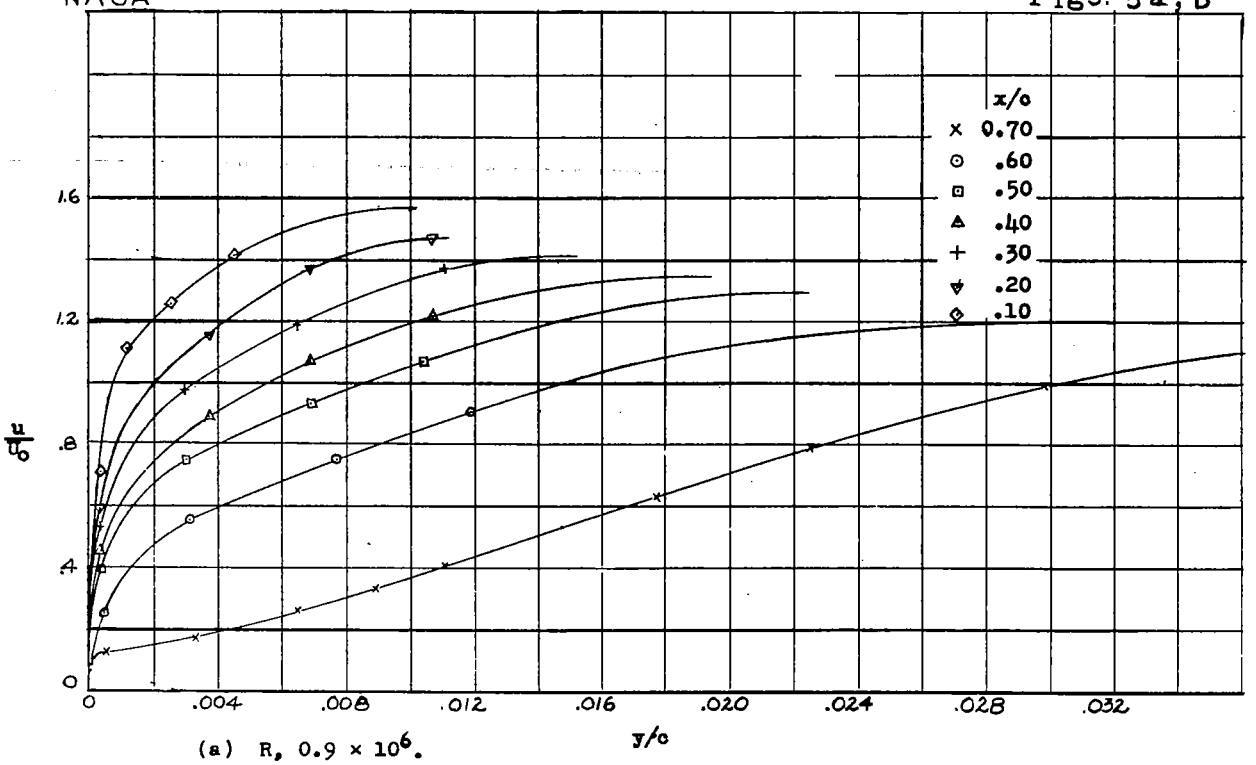

(a) R, 0.9×10^6.

Figure 5.- Boundary-layer velocity profiles in the region from the 10-percent-chord to the 70-percent-chord stations. NACA 66,2-216, a = 0.6, airfoil section; α, 10.1°.

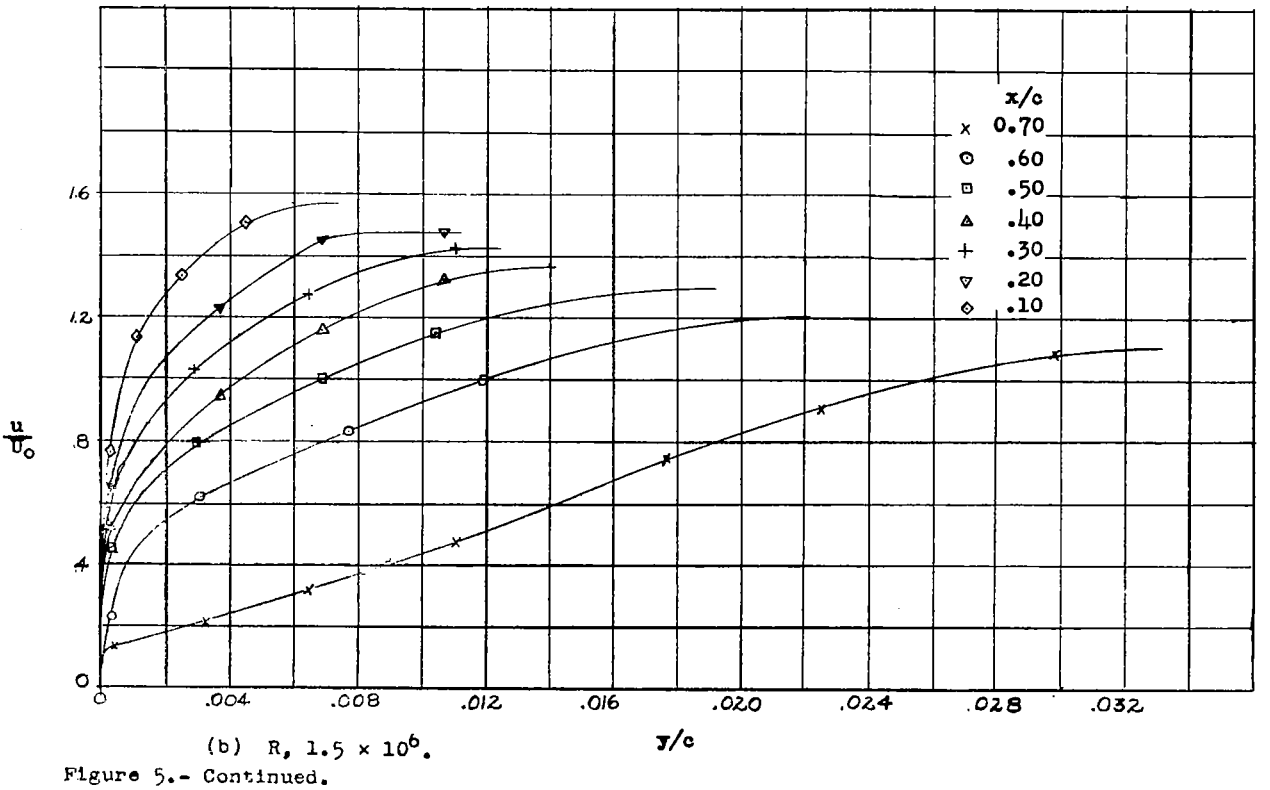

(b) R, 1.5×10^6.

Figure 5.- Continued.

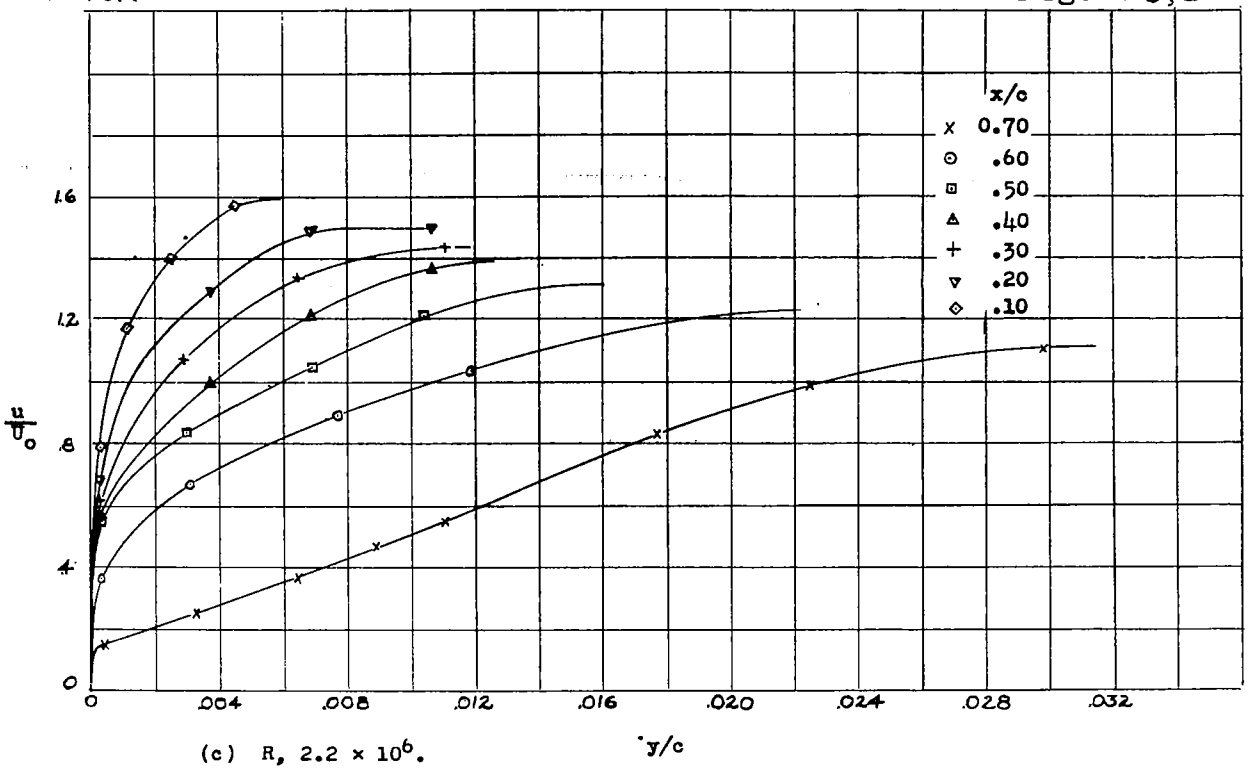

(c) R, 2.2×10^6.

Figure 5.- Continued.

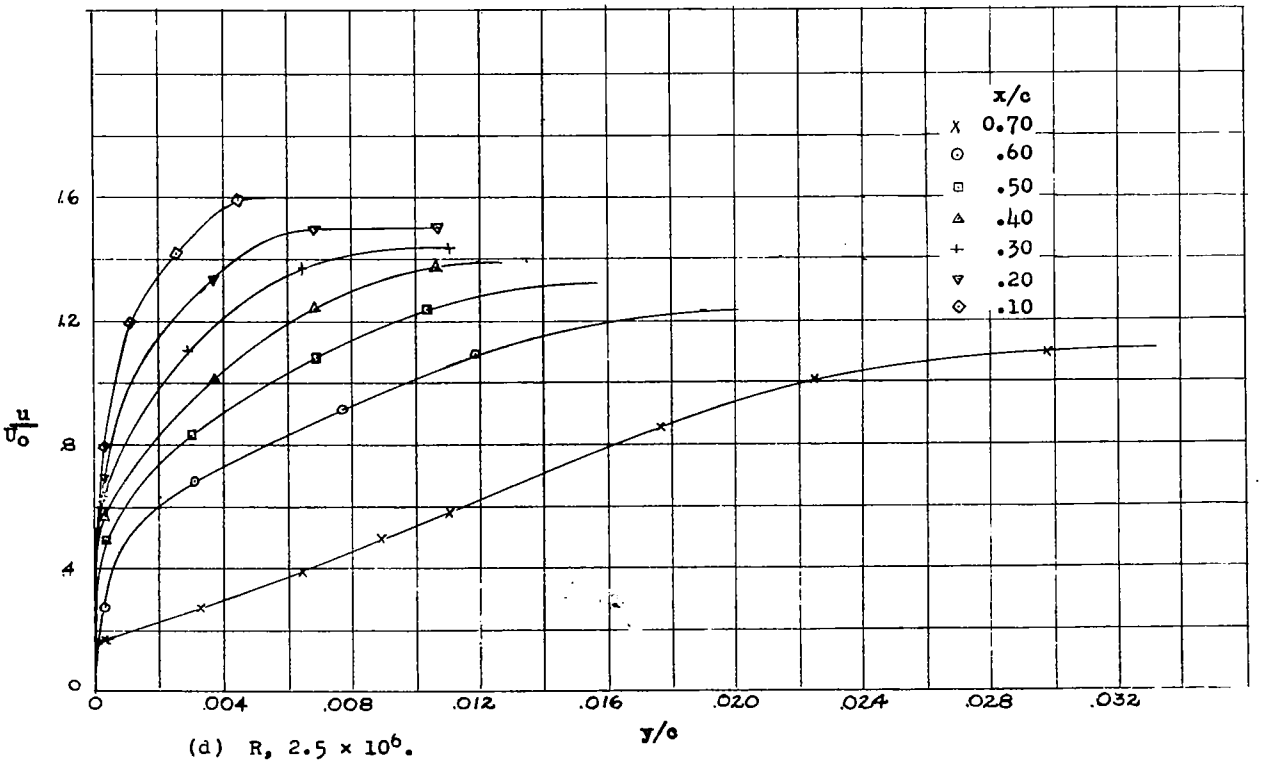

(d) R, 2.5×10^6.

Figure 5.- Concluded.

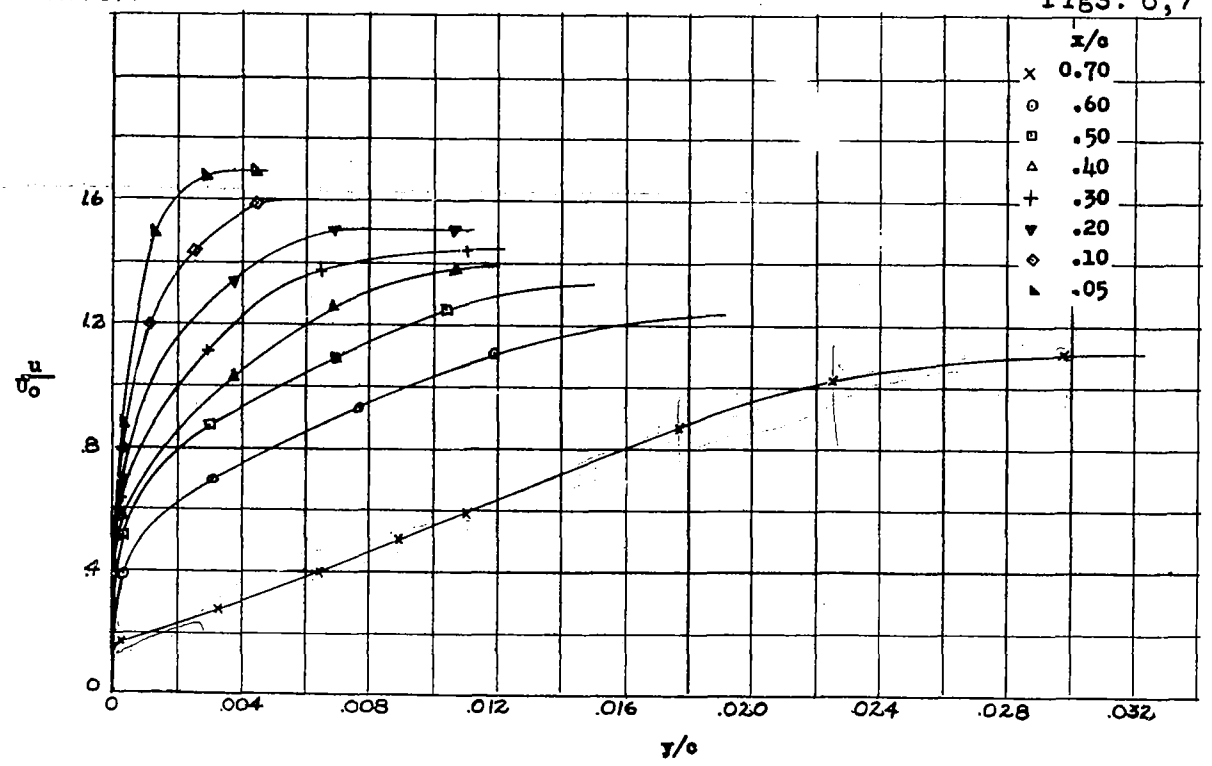

Figure 6.- Boundary-layer velocity profiles in the region from the 5-percent-chord to the 70-percent-chord stations. NACA 66,2-216, $a = 0.6$, airfoil section; α, 10.1°; R, 2.6×10^6.

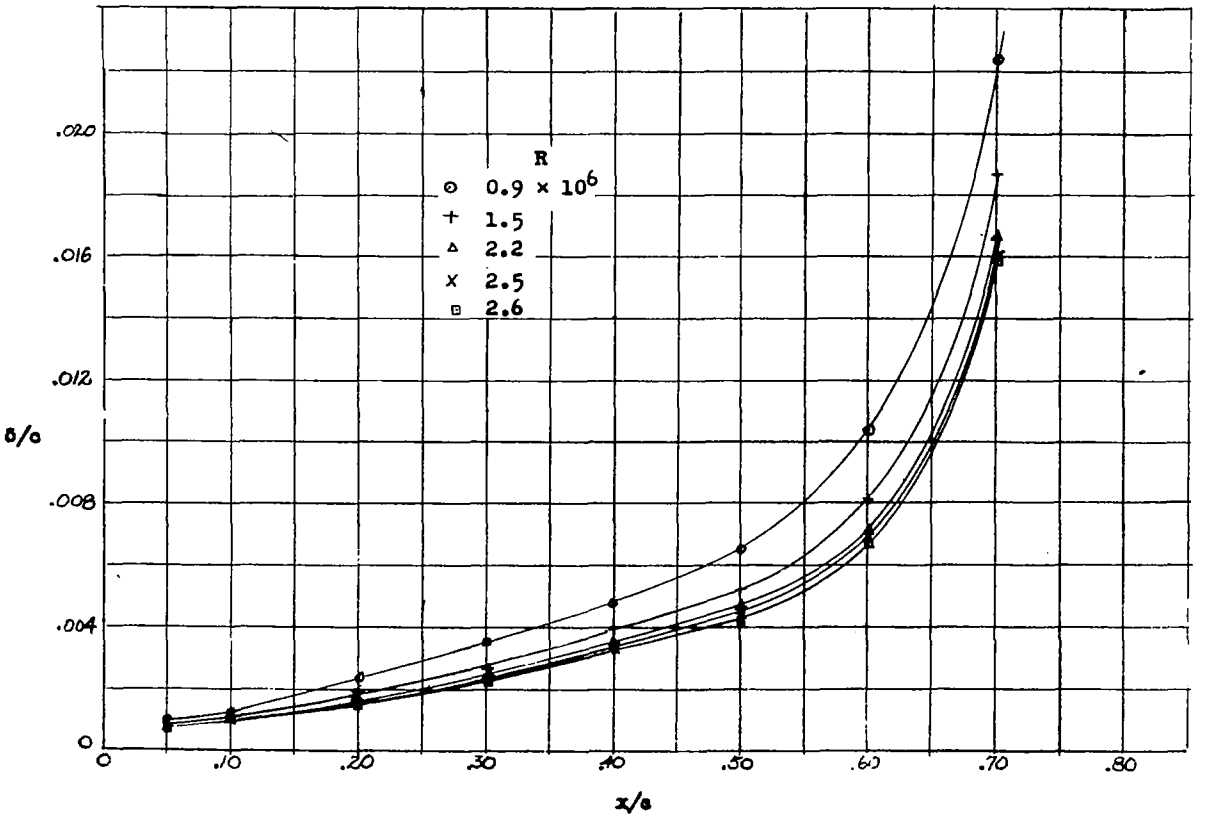

Figure 7.- Variation of boundary-layer thickness with chordwise position for various Reynolds numbers. NACA 66,2-216, $a = 0.6$, airfoil section; α, 10.1°.

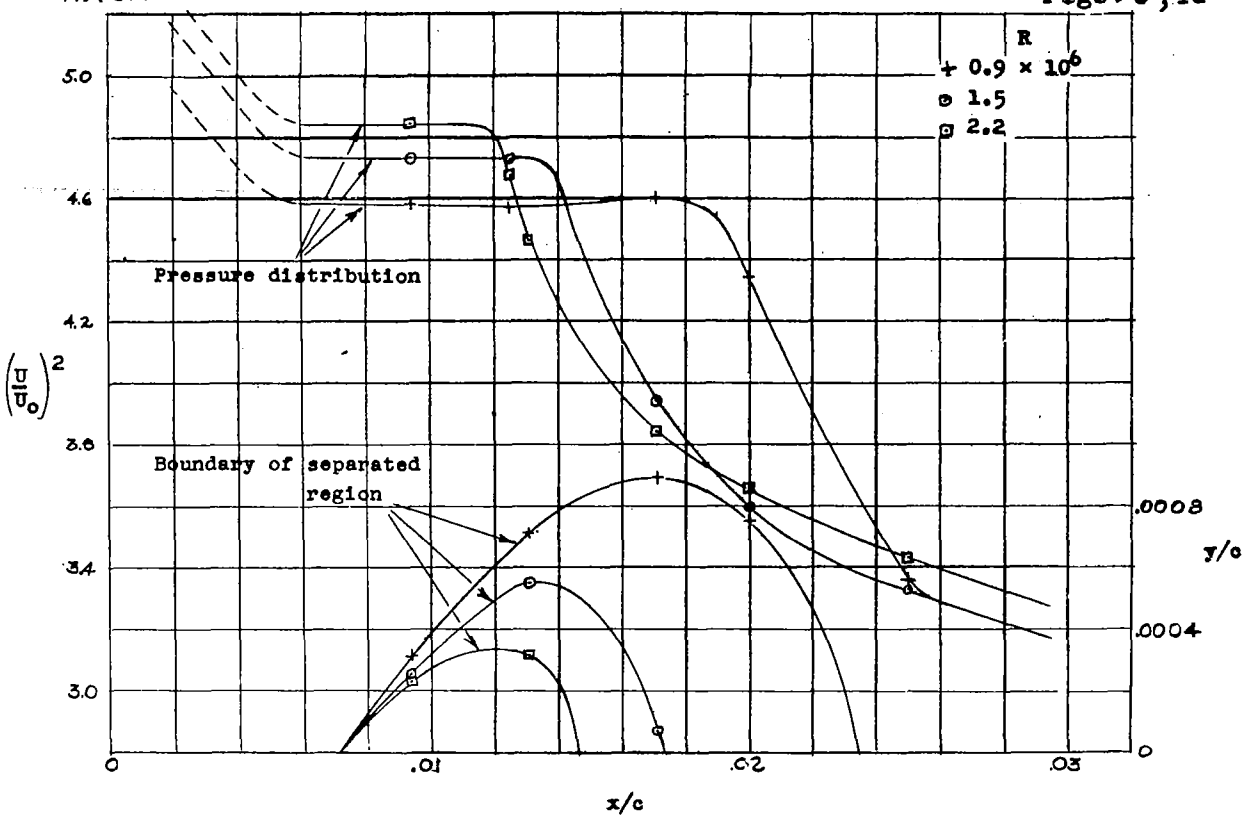

Figure 9.- Extent of separated region and pressure distribution near leading edge of NACA 66,2-216, a = 0.6, airfoil section. α, 10.1°.

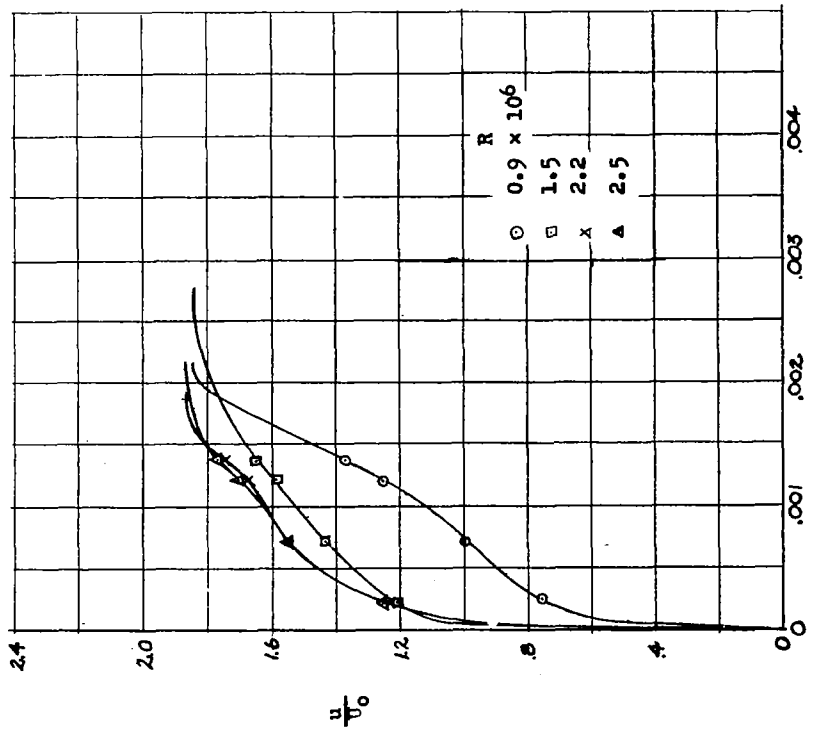

Figure 11.- Boundary-layer velocity profiles at the 2.5-percent-chord station, NACA 66,2-216, a = 0.6, airfoil section; α, 10.1°; x/c, 0.025.

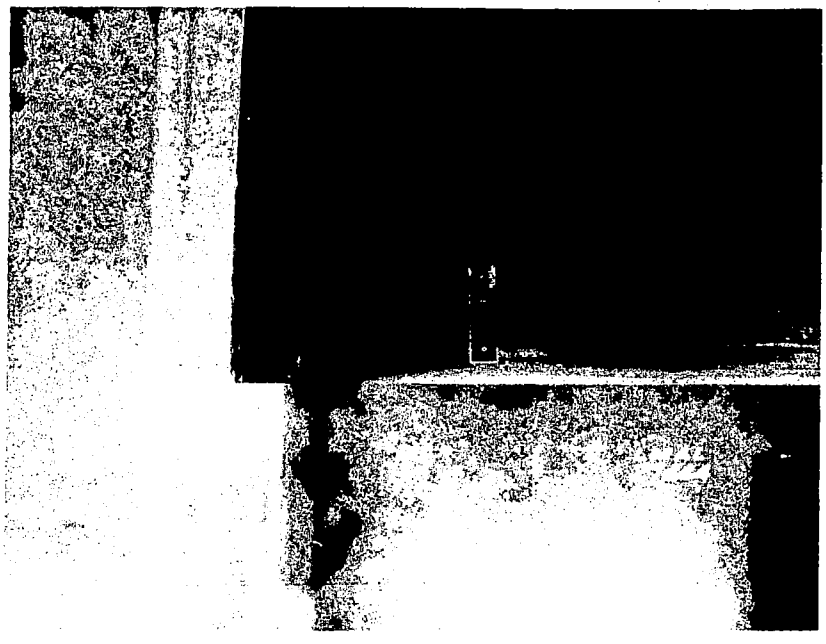

(a) Model before tunnel was started.

Figure 10(a to e).- Suspension of lampblack in kerosene painted on upper surface near leading edge of NACA 66, 2-216, $a = 0.6$, airfoil section. α, 10.1. Direction of flow from bottom to top of photographs.

(b) Flow pattern at R = 0.9 x 10^6.

(c) Flow pattern at R = 1.5 x 10^6.

Figure 10.- Continued.

(d) Flow pattern at $R = 2.2 \times 10^6$.

(e) Flow pattern at $R = 2.5 \times 10^6$.

Figure 10.- Concluded.